Immobilization of Yeast on Magnetic Nano Supports for Biotechnological Applications in the Bioethanol Industry

Neidelênio Baltazar Soares , Symone Costa de Castro , João Guilherme M. Pontes , Ljubica Tasic *

Posted Date: 26 May 2026

doi: 10.20944/preprints202605.1727.v1

Keywords: yeast immobilization; magnetic nanoparticles; *Saccharomyces cerevisiae*; bioethanol

 doi:10.20944/preprints202605.1727.v1

Article

Immobilization of Yeast on Magnetic Nano Supports for Biotechnological Applications in the Bioethanol Industry

Neidelênio Baltazar Soares, Symone Costa de Castro, João Guilherme M. Pontes and Ljubica Tasic *

Chemical Biology Laboratory, Institute of Chemistry, Organic Chemistry Department, Universidade Estadual de Campinas, Rua Monteiro Lobato, 270, Campinas, São Paulo, Brazil

* Correspondence: ljubica@unicamp.br

Abstract

The development of support for the immobilization of enzymes and yeasts is an important step in hydrolysis and fermentative processes, aiming to recover and reuse biocatalysts, thereby making the process of bioethanol production economically viable. In this study, we propose a core/shell support made of nanomagnets armed with *Saccharomyces cerevisiae* cells as a nanobiocatalyst for fermentative processes. We use orange biomass, a common waste in Brazil, for bioethanol production. The produced nanomagnets had a zeta potential of +28.0 ± 0.5 mV, were efficiently covered by silica and armed with -NH_2 groups, and were duly characterized by infrared spectroscopy. The biomass after acid hydrolysis presented 10 ± 0.6 g L^{-1} of reducing sugars, which were quantified using the colorimetric method. An evaluation of fermentation conditions was carried out by varying temperature and pH. In the first condition, the achieved ethanol yield was 35-46% after 48 h of fermentation, while in the second condition, we obtained 48-90% ethanol, and in the third condition, 50-69.2%. The produced bioethanol was quantified through a chemical oxidation reaction. The immobilization process proved to be satisfactory with a reaction yield of around 25-30%.

Keywords: yeast immobilization; magnetic nanoparticles; *Saccharomyces cerevisiae*; bioethanol

1. Introduction

The reduction in the use of fossil fuels faces global regulatory barriers, despite the proven viability of biofuels. The transition to renewable energy sources can reduce costs and mitigate greenhouse gas emissions [1–5]. Faced with these challenges, it is imperative to seek new, low-carbon, alternative energy sources in order to sustain a high standard of sustainable development. In this context, it is crucial to develop innovative methods for efficient energy use [6–9]. These methods, in turn, must provide energy from renewable and clean sources, while reducing environmental pollution and not compromising food security [10,11]. Biofuels, which are fuels generated from renewable raw materials [12], are generally classified into different types, such as first (1G), second (2G), third (3G), and fourth (4G) generation biofuels [13]. First-generation biofuels use edible biomass such as starch and sugar [8,10]. While those of the second generation (2G) are based on the use of the most efficient renewable alternatives, using non-edible lignocellulosic biomass for human consumption, Third-generation (3G) biofuels are derived from marine biomass, particularly algae. In contrast, fourth-generation (4G) biofuels employ genetically engineered microorganisms capable of fixing high concentrations of CO_2 [9,10]. Ethanol is an example of a biofuel produced on a large scale in Brazil, which is produced mainly from sugar cane [14]. Ethanol is the main representative source of bioenergy [15]. Over the past 10 years, global ethanol production has seen consistent growth, with an average annual increase of 3.8%. In 2023, this growth reached a notable peak, reaching the impressive mark of 115 billion liters of this biofuel [16]. Despite the high yield of first-generation

 doi:10.20944/preprints202605.1727.v1

ethanol, there is a strong dependence on food crops such as corn and sugarcane, where production technologies are more consolidated. However, this type of ethanol faces competition challenges with food supply and land use [10,17]. 2G ethanol was developed to solve the limitations presented by 1G bioethanol, using mainly inedible cellulosic biomass [8,18]. Among the plant sources used for the production of second-generation ethanol (2G ethanol), a variety of agricultural residues stand out [19–21]. These include corn straw and other cereals, husks, and bagasse from various crops, such as sugar cane, orange, eucalyptus, soybeans, and corn, which are also used in the production of 2G ethanol [21,22]. Lignocellulosic biomass has significant potential to become a highly competitive raw material in the generation of renewable energy or in the production of value-added biomolecules [23]. The use of biomass as an energy source has several advantages, such as the reduction of CO_2 emissions, and it contributes to mitigating the effects of climate change [24]. Regarding its constitution, lignocellulosic biomass is mainly composed of two types of carbohydrate polymers, cellulose and hemicellulose, and a non-carbohydrate phenolic compound called lignin [25,26]. Biomass generated from the processing of citrus fruits is a viable alternative to lignocellulosic biomass for the production of 2G ethanol, since Brazil is the largest exporter of orange juice, which means that a large part of the fruits produced are industrially processed for juice production. Orange biomass differs from others, since the main polysaccharide present is pectin (between 30-35% on a dry basis), while cellulose and hemicelluloses are present in smaller quantities, and lignin is a minor component. Currently, 80% of the oranges produced in Brazil are destined for the production of juice and juice concentrate, which means that the amount of waste generated by orange processing is huge. In fact, the forecast for processed oranges in Brazil was around 69% of total production in 2020, which impacts the environment [27,28]. The residue that is generated from juice processing is normally called orange peel waste (OPW), and it consists of peels, seeds, and pulp. OPW is generally transformed into "pellets", which can be used for animal feed [29,30]. Another possibility for OPW, in addition to being used as animal feed, consists of its use to produce 2G ethanol [22]. Once hydrolyzed, polysaccharides present in OPW biomass are easily fermented by yeast, producing this biofuel. This innovative use of orange peel not only takes advantage of a common waste product from the orange juice industry but also contributes to the production of renewable biofuels, reducing dependence on fossil energy sources and promoting a more sustainable economy [31]. The processing of OPW to obtain alcohol has been increasingly adopted as a lignocellulose raw material subjected to simultaneous saccharification and fermentation (SSF) for the production of bioethanol [32–34]. The *S. cerevisiae* is the yeast widely used in several areas such as the ethanol industry, baking, beer making, and winemaking [35,36], due to its inherent ability to produce high amounts of ethanol, tolerance to low pH, high concentrations of sugar and ethanol, and resistance to some inhibitors released from lignocellulosic hydrolysates [22,37,38]. During the alcoholic fermentation process, some factors such as increased temperature, change in pH, osmotic stress, and ethanol concentration can cause stress in *S. cerevisiae*, which, in turn, will affect ethanol production [39]. A range between 20–35 °C is acceptable for *S. cerevisiae* with an optimal growth temperature of 30 °C, while an increase to approximately 40 °C induces the biosynthesis of stress response factors such as heat shock proteins, this is why it is essential to maintain temperature control [40]. One of the most significant challenges in fermentation is the inhibition of yeast cell growth due to ethanol accumulation. The development of an immobilization technology to separate and reuse yeast cells from the fermentation medium can be considered a promising method to mitigate toxicity and cell mortality [41]. A viable alternative to control the morphological structure of these microorganisms is cell immobilization (CI). This technique aims to maintain the necessary catalytic activity, being applicable in both laboratory and industrial environments [42]. The use of immobilization techniques is an effective strategy to solve problems associated with enzymes and free yeast in terms of improving the efficiency, stability, and yield of the process [37,41,43]. An alternative used in fermentation processes is the immobilization of yeast in materials such as DEAE-cellulose, calcium alginate, calcium pectate, or sintered glass. Immobilization increases the biomass per unit of reactor volume in a shorter time [44]; however, the selection of a suitable matrix for cell immobilization is crucial to obtain the desired product, being a

 doi:10.20944/preprints202605.1727.v1

specific decision for each microorganism and metabolite under study [45,46]. The main limitation of this method is the possibility of cell separation due to the low intensity of stabilization forces [47,48]. A promising alternative to this problem consists of the use of magnetic nanoparticles coated with silica, as they facilitate the separation of the reaction medium through the use of magnets, when it is necessary to regenerate the bioreactor substrate, while silanes have ordered pore diameters, whose size can be targeted to adequately protect target yeasts and enzymes [41,49,50]. The immobilization of microbial cells on solid supports depends on molecular forces such as electrostatic, ionic, van der Waals, hydrogen bonding, hydrophilic, and hydrophobic interactions. However, due to the reversible nature of these interactions, cell detachment is a significant disadvantage of this method. To avoid desorption of microorganisms from the matrix, it is crucial to promote strong adsorption between cells and support. This can be achieved by tuning the support characteristics (such as particle size, porosity, specific area, charge), chemically modifying the support surface to increase favorable interactions (e.g., introducing reactive groups such as $–NH_2$,—OH, –COOH, –SH), or by the use of combined materials [51,52].

Magnetic iron nanoparticles are widely used in the area of biotechnology, mainly as a support for the immobilization of enzymes and yeast, offering the opportunity to reduce working time, process cost, and the possibility of reuse, and can be used in continuous systems [41,53]. In the M-IONPs family of magnetic nanoparticles, the three most common types are magnetite (Fe_3O_4), maghemite (γ-Fe_2O_3). and hematite (α-α-Fe_2O_3). Hematite (α-Fe_2O_3) is known for its high chemical stability when exposed to air for prolonged periods [54].

The focus of this article is the optimization of fermentation bioprocess, where hydrolyzed sugars from OPW are converted into ethanol through the action of the yeast *S. cerevisiae*, It is proposed to evaluate the potential of Fe_3O_4 magnetic iron nanoparticles, coated with inert material, and functionalized for the immobilization of *S. cerevisiae* yeast cells during the ethanol production process using orange pomace as a source of sugars and, as an alternative acid hydrolysis. Figure 1 illustrates the complete process from the synthesis of the magnetic nanoparticles (MNP), cellular immobilization, and application in fermentation processes.

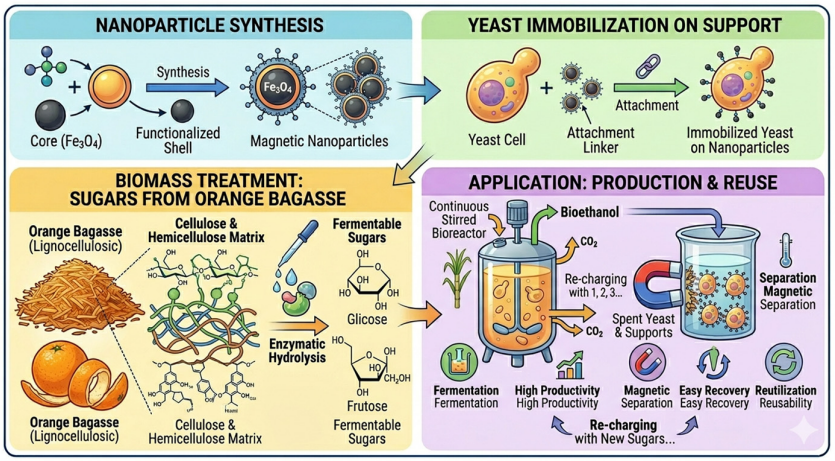

Figure 1. Illustration of steps of MNP synthesis, cellular immobilization, and application in fermentation. Figure generated in AI Gemini.

2. Materials and Methods

2.1. Synthesis of Fe_3O_4 Nanoparticles

The procedure for MNP synthesis was adapted from the methodology described by Oberacker et al. [55] and carried out in our research laboratory with some adaptations. The coprecipitation method was used. To this end, an aqueous solution of Fe^{2+}/Fe^{3+} was prepared in a 1:2 molar ratio. The

 doi:10.20944/preprints202605.1727.v1

salts used were $FeSO_4 \cdot 7H_2O$ and $FeCl_3 \cdot 6H_2O$. Then, they were slowly dripped into the flask containing 100 mL of an alkaline sodium hydroxide solution (NaOH 2 mol L^{-1}) heated between 70 and 80 °C, under stirring (400 to 500 rpm). The nanoparticles were magnetically separated after cooling to room temperature, then repeatedly purified with ethanol (2x) and water (2x) and stored at room temperature under vacuum. The synthesis was carried out in triplicate, until the MNP were obtained under the same working conditions after synthesis, the pH of the nanoparticles was around 11, washing allowed the pH to be 7. Then, gravimetry was carried out to determine the quantity obtained. The MNPs were stored in an evacuated desiccator until the next stage.

2.2. Surface Modification with TEOS and APTES

Fe_3O_4 MNP coating was adapted from Oberacker et al., 2019 [55]. 2.5 g of Fe_3O_4 MNP was mixed with 200 mL of ethanol. The suspension was dispersed in an ultrasonic bath for 30 min. A solution containing 2 g tetraethyl orthosilicate (TEOS), 50 mL ethanol, and 6 mL ammonia (NH_3, 25% *v*/*v*) was added. Vigorous stirring was maintained in a 25 °C water bath for 4 h. The Fe_3O_4@SiO_2 were washed with water (3–4 times), twice with ethanol, and dried under vacuum at room temperature. For the amino functionalization, 150 mg of Fe_3O_4@SiO_2 were suspended in 30 mL of water, and 0.6 mL of 3-aminopropyltriethoxysilane (APTES) was added. The suspension was maintained at 70 °C for 16 h under vigorous stirring. The Fe_3O_4@SiO_2 –NH_2 was washed with water (3–4 times), twice with ethanol, and dried under vacuum.

2.3. Nanoparticles Characterisation

The zeta potential (ζ) and hydrodynamic radius were measured using 0.01 mg mL^{-1} water suspensions in a DST1070 folded cuvette in a Zetasizer Nano-ZS (Malvern). Size and shape were determined by Transmission Electron Microscopy in a Carl Zeiss CEM-902 with 80 keV using copper grids and parlodium film. The microscope was equipped with a Castaing-Henry-Ottensmeyer filter spectrometer used for the electron energy loss spectrometry (EELS). The crystal structure was determined by X-ray Diffraction (XRD) using a D2-Phaser Bruker from IFGW—DEQ-l 108 (UNICAMP), operating with 30 kV, current: 10 mA, radiation: Cu 1.54184 angs., continuous scanning mode, time per step: 0.4 s, range (2 theta) : 5°–80°, increment of 0.02°; linear detector (LYNXEYETM); usage time: 1.5 h. Surface functionalization was investigated by Infrared Spectroscopy equipped with Attenuated Total Reflectance (ATR-FT-IR) using an Agilent Cary 630. X-Ray Photoelectron spectra were obtained using a SPECS system (SPECS GmbH) equipped with X-ray XR-50 with radiation Al Kα (hν = 1486.6 eV) and Phoibos 100 analyser with MCD-9 detector at the CCS Nano laboratory (Centro de Componentes Semicondutores, UNICAMP).

2.4. Chemical Composition of Orange Peel Waste (OPW)

Moisture of the dry OPW samples was determined based on the US National Renewable Energy Laboratory (NREL)'s standard procedure [56]. The ash content was determined using AOAC methods (AOAC, 2016) [57]. Pectin was extracted and analyzed according to the literature [7]. Acid detergent fiber (ADF), neutral detergent fiber (NDF), and acid detergent lignin (ADL) were determined with ANKOM Technology Methods [58]. All analyses were performed in triplicate.

2.5. Acid Hydrolysis of Orange Pomace and Sugar Quantification

250 mL Erlenmeyer flasks containing 17.0 g of orange pomace residue were prepared, then distilled water and sulfuric acid (98%) were added, reaching a concentration of 0.5% (*m*/*v*) at a final volume of 100 mL. Then, the samples were heated in an autoclave at 120 °C (15 or 30 min). The hydrolysates were analyzed for reducing sugars using 3,5-dinitrosalicylic acid (DNS). The treatment allowed us to obtain hydrolysates with a higher sugar content, which were then stored and used in the fermentation experiment. All experiments were performed in triplicate. The sugars were quantified using a calibration curve, as shown in the attachment in Supplementary Table S1.

 doi:10.20944/preprints202605.1727.v1

2.6. Microorganism and Culture Media

Commercial yeast (*S. cerevisiae* brand Fleischmann), purchased from the local market, was prepared in sterilized Erlenmeyer flasks (250 mL) in a medium containing Yeast Extract-Peptone-Dextrose 2% (YPD), 10.8 g L^{-1} of yeast extract, 15 g L^{-1} of peptone, and 20 g L^{-1} of dextrose (D-Glucose), and chloramphenicol (30 ug mL^{-1}) was added. The vials were incubated at 30 °C for 24 h in a shaker shaking at 120 rpm. The inoculum was transferred to sterile Erlenmeyer flasks (250 mL) containing 100 mL of YPD medium with 30 ug mL^{-1} of chloramphenicol.

2.7. Yeast Immobilization on Magnetic Nanoparticles

For the immobilization process, the magnetic nanoparticles were dispersed in a sodium phosphate solution (pH 4.5) and stored for 12 h at room temperature. Then, fresh yeast cells were washed three times with 0.9% NaCl saline to remove the culture medium. The cells were then mixed with an equal volume of MNP and shaken in a shaker incubator for 24 h at 35 °C to allow the nanoparticles to adhere to the surface of the cells. The immobilized cells were then transferred to the fermentation medium. The immobilization efficiency was examined by exposing the immobilized cells to a magnetic field. After 5, 10, 15, 20, and 25 min, the supernatants were collected and inoculated onto the LB agar plates. The resulting colonies were counted after 24 h of incubation at 30 °C, and the immobilization efficiency was calculated based on Equation (1).

$$Ei = \frac{CFUt0 - CFUt1}{CFUt0} * 100 \quad (1)$$

where E_i is the immobilization efficiency and CFU_{t0} and CFU_{t1} are the number of colonies obtained before and after exposure to the magnetic field, respectively

2.8. Fermentation Process

The fermentation process illustration is shown in Figure 2.

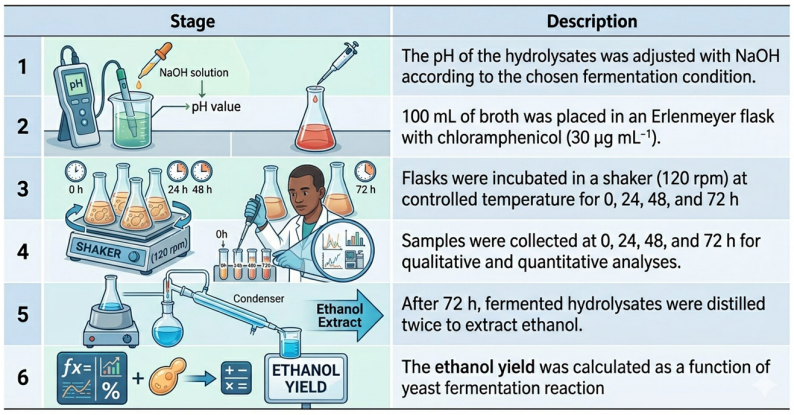

Figure 2. Summary of the protocol of the fermentation process of *S. cerevisiae*.

2.9. Quantification of Ethanol Using the Colorimetric Method

Ethanol quantification was performed using a standard curve with ethyl alcohol (PA, Dinâmica). Standard ethanol solutions were prepared in the range of 1.6–12.8 mg mL^{-1}. 5 mL of sodium dichromate solution (40 mg mL^{-1}) was added, and 15 mL of standard solution was added. Then, 25 mL of H_2SO_4 solution. The pH of the solution was maintained by 0.2 mol L^{-1} of acetate buffer with a pH value of 4.3. Then, the mixture was stirred for 1 min and incubated for 2 h. After this, a green product was observed, the absorbance of the solutions was taken at 578 nm, and based on the

 doi:10.20944/preprints202605.1727.v1

readings, the standard curve was constructed. The experimental samples were treated in the same way, followed by absorbance measurement, and the ethanol concentration was determined from the standard curve according to Supplementary Table S2.

3. Results

3.1. Synthesis and Characterization of Nanoparticles

The synthesis of MNPs—magnetic nanoparticles (Fe_3O_4) was performed using the co-precipitation method, which can be described by Equation (2).

$$Fe^{2+} + 2Fe^{3+} + 8OH^- \rightarrow Fe_3O_4 + 4H_2O \quad (2)$$

The synthesized nanoparticles exhibited strong magnetic responsiveness in the presence of a permanent magnet (Figure 3).

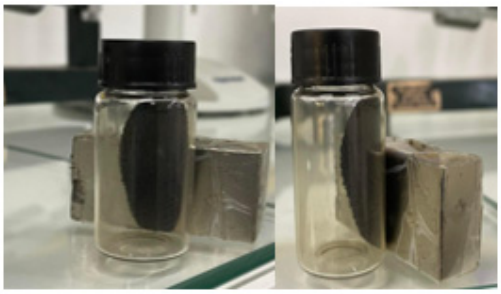

Figure 3. Magnetic nanoparticles in the presence of a permanent magnet.

Elemental analysis (CHN) revealed a progressive increase in carbon, hydrogen, and nitrogen content after each modification step, confirming the successful coating and functionalization of the nanoparticles (Table 1).

Table 1. Elemental analysis of magnetic nanoparticles (MNPs).

Samples	% Carbon	% Hydrogen	% Nitrogen
Fe_3O_4	0.17	0.37	0.00
$Fe_3O_4@SiO_2$	0.26	0.37	0.17
$Fe_3O_4@SiO_2@NH_2$	6.31	2.12	1.44

The average hydrodynamic diameter increased from 244.4 ± 1.0 nm for Fe_3O_4 to 368.0 ± 0.4 nm for $Fe_3O_4@SiO_2$ and 399.0 ± 0.5 nm for $Fe_3O_4@SiO_2@NH_2$ (Table 2). Correspondingly, zeta potential values changed from +22.0 ± 0.8 mV to −28.0 ± 0.5 mV after silica coating and to +35.0 ± 0.2 mV after APTES functionalization.

Table 2. Size of magnetic nanoparticles (MNPs) and zeta potential.

Samples	Average Diameter (nm)	Zeta Potential (mV)
Fe_3O_4	244.4 ± 1.0	+22.0 ± 0.8
$Fe_3O_4@SiO_2$	368.0 ± 0.4	-28.0 ± 0.5
$Fe_3O_4@SiO_2@NH_2$	399.0 ± 0.5	+35.0 ± 0.2

Transmission electron microscopy (TEM) images (Figure 4) showed average particle diameters of 27.00 ± 0.01 nm for Fe_3O_4, 35.00 ± 3.21 nm for $Fe_3O_4@SiO_2$, and 115.00 ± 7.52 nm for $Fe_3O_4@SiO_2@NH_2$.

 doi:10.20944/preprints202605.1727.v1

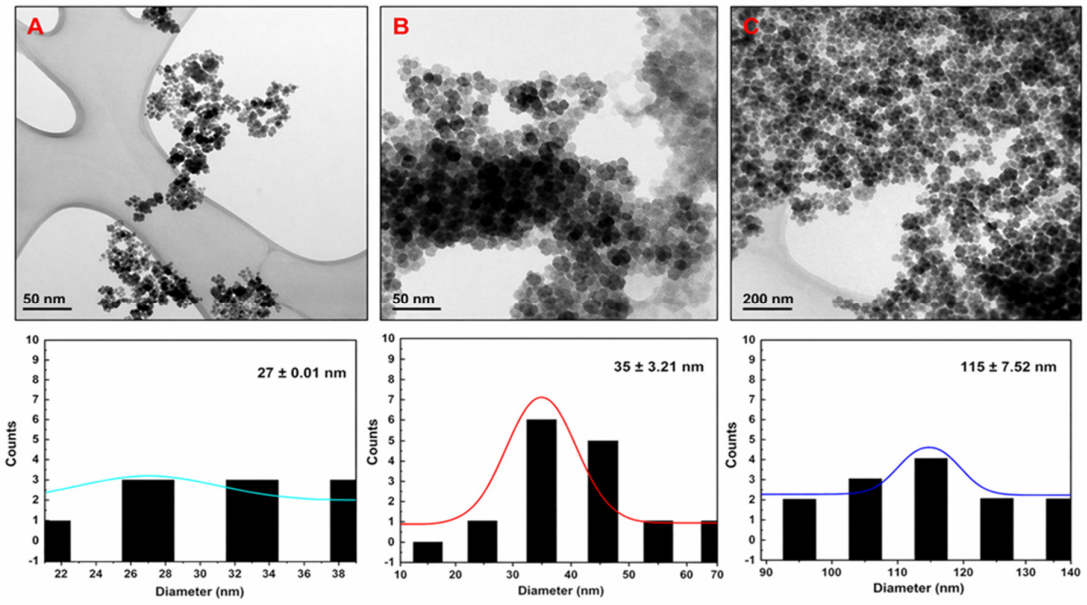

Figure 4. TEM images illustrating the structural and morphological evolution of nanoparticles during the synthesis process: (A) Fe_3O_4, (B) Fe_3O_4@SiO_2, and (C) Fe_3O_4@SiO_2–NH_2. The particle size distribution histograms (bottom) confirm mean diameters of 27 ± 0.01 nm, 35 ± 3.21 nm, and 115 ± 7.52 nm, respectively.

FT-IR spectra (Figure 5) confirmed the formation of Fe_3O_4 by characteristic bands at 440 and 568 cm^{-1}. Additional bands at 1058 and 960 cm^{-1} verified the presence of silica, while bands at 1490 and 690 cm^{-1} confirmed the successful incorporation of amine groups after APTES functionalization.

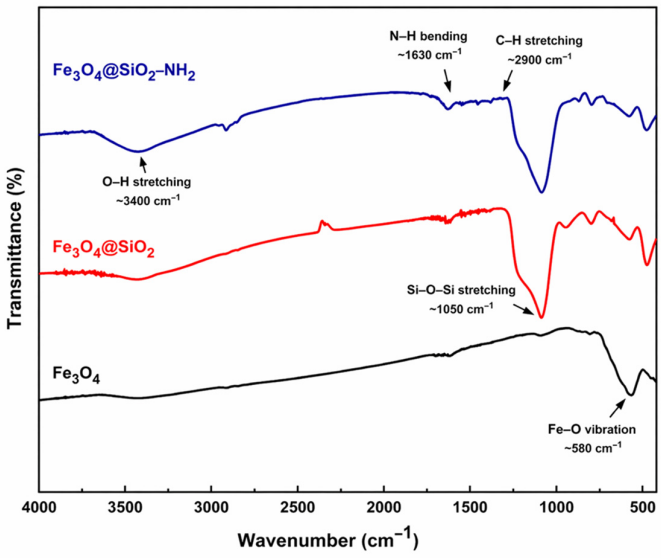

Figure 5. FT-IR spectra of solid samples of magnetic nanoparticles of: Fe_3O_4 (in black), Fe_3O_4@SiO_2 (in red), Fe_3O_4@SiO_2-NH_2 (in blue).

3.2. Composition of Orange Peel Waste (OPW)

OPW presented a moisture content of 80.48 ± 2.30% and an ash content of 5.74 ± 0.06%. The lignocellulosic fraction consisted of 15.88 ± 1.68% hemicellulose, 19.73 ± 0.70% cellulose, and 5.96 ± 0.68% lignin. Additionally, the material contained 19.52 ± 2.30% total solids, 13.94 ± 0.78% ADF, and 29.24 ± 2.24% NDF.

 doi:10.20944/preprints202605.1727.v1

3.3. Efficiency of Cell Immobilization

Figure 6 shows the interaction between Fe_3O_4@SiO_2@NH_2 nanoparticles and *Saccharomyces cerevisiae* cells, resulting in a visible darkening of the yeast suspension, indicating nanoparticle attachment.

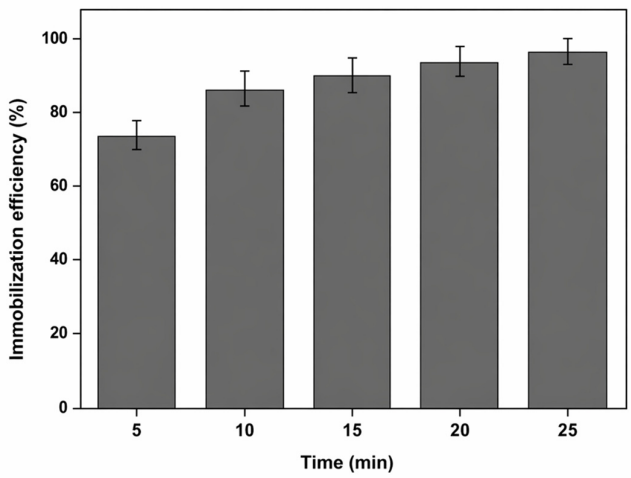

Figure 6. Time-dependent profile of yeast immobilization efficiency (%) onto magnetic nanoparticles, showing a gradual increase in immobilization yield from 5 to 25 min. Data are expressed as mean ± standard deviation.

3.4. Hydrolysis and Fermentation with Free Yeast

The hydrolysis of orange bagasse generated fermentable sugars that were subsequently converted to ethanol by free *S. cerevisiae*. At pH 4.0 and 28 °C, ethanol production increased up to 48 h, reaching a maximum yield of 56%. At pH 4.5 and 30 °C, the highest fermentation performance was observed, with a maximum ethanol yield of 90% after 48 h. At pH 5.0 and 35 °C, despite substantial glucose consumption, ethanol production was lower and decreased after 72 h (Figure 7)

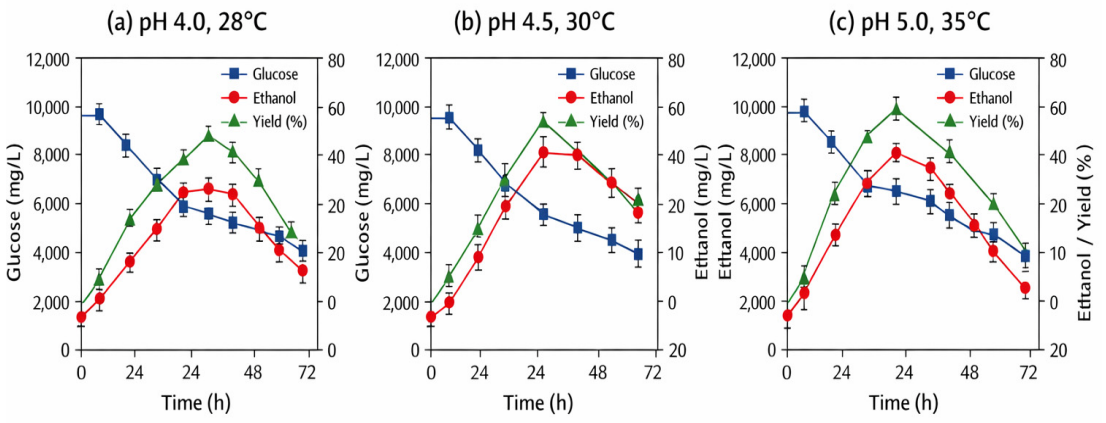

Figure 7. Comparative fermentation kinetics showing glucose consumption (mg L^{-1}), ethanol production (mg L^{-1}), and yield (%) over time using free *S. cerevisiae* at (a) pH 4.0 (28 °C), (b) pH 4.5 (30 °C), and (c) pH 5.0 (35 °C), monitored over 72 h.

3.5. Hydrolysis and Fermentation with Yeast Immobilized on Magnetic Iron Nanoparticles

Immobilized yeast on magnetic nanoparticles maintained stable performance over six consecutive fermentation cycles (Figure 8). After 24 h, ethanol yields were approximately 9.2–9.8%.

 doi:10.20944/preprints202605.1727.v1

At 48 h, yields increased to 29–31.4%. After 72 h, yields decreased to 22–24%. These results demonstrate the operational stability and reusability of the Yeast@MNP system.

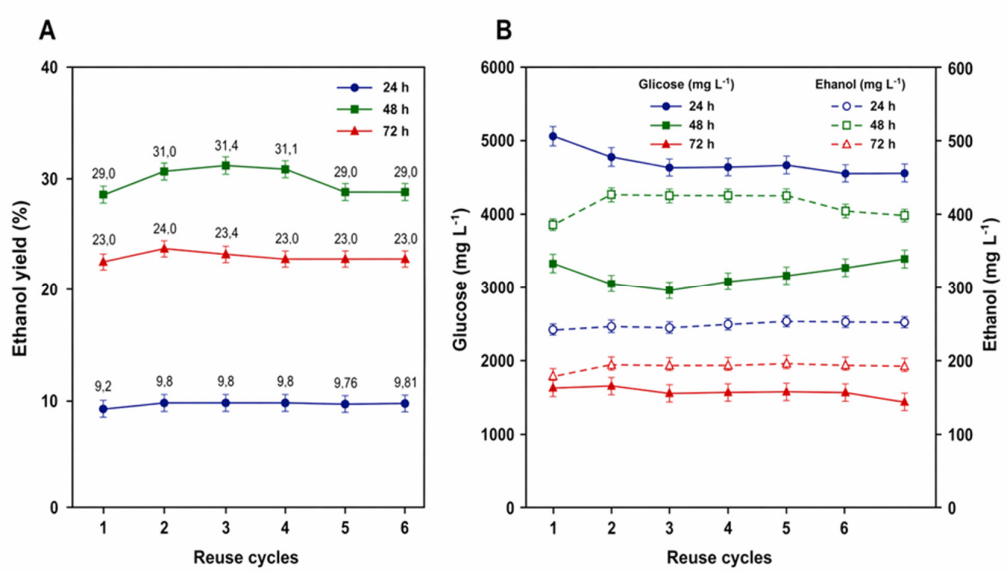

Figure 8. Ethanol production performance of immobilized *S. cerevisiae* on magnetic nanoparticles over six (6) consecutive fermentation cycles. (A) Ethanol yields (%) after 24, 48, and 72 h of fermentation. (B) Glucose concentration (mg L^{-1}, solid lines) and ethanol concentration (mg L^{-1}, dashed lines) during the reuse cycles.

4. Discussion

The co-precipitation method was selected due to its operational simplicity, high efficiency, good reproducibility, and economic viability. Furthermore, it is a fast and direct approach for obtaining nanoparticles, which can be conducted under relatively mild temperature conditions (generally around 70 °C), which favors the control of particle size and properties [55,59]. Figure 2 illustrates the nanoparticles in the presence of a permanent magnet.

The progressive increase in CHN content confirms the successful incorporation of silica and aminosilane layers, consistent with previous findings reported by our research group (2021) [60].

The increase in hydrodynamic diameter after each modification step, together with the inversion of zeta potential, provides strong evidence of effective surface engineering. The negative surface charge after silica coating is attributed to deprotonated silanol groups, whereas the positive charge observed after APTES functionalization reflects protonated amino groups [49,60–62].

The high cellulose and hemicellulose contents demonstrate the suitability of OPW as a renewable feedstock for second-generation bioethanol production. The relatively low lignin content is advantageous because it reduces biomass recalcitrance and facilitates hydrolysis and fermentation.

The rapid immobilization kinetics, with 98% attachment within 25 min, indicate a strong interaction between positively charged amino-functionalized nanoparticles and negatively charged yeast cell surfaces.

This result is superior to that reported by Firoozi et al. (2022) [41], who obtained 91% immobilization after 20 min.

The results confirm the critical influence of pH and temperature on ethanol production. The best performance at pH 4.5 and 30 °C agrees with the optimal growth conditions commonly reported for *S. cerevisiae* [12,63–65]. Reduced ethanol production at 35 °C likely reflects thermal stress and enhanced formation of byproducts.

The gradual increase in ethanol yield from 24 to 48 h suggests adaptation of immobilized cells and improved metabolic activity.

 doi:10.20944/preprints202605.1727.v1

The decrease observed after 72 h may be attributed to substrate depletion, ethanol accumulation, and diffusional limitations. Compared with traditional supports such as calcium alginate [66], MNP offers several advantages, including easier recovery, lower mass-transfer resistance, and improved process control.

The stability observed over six fermentation cycles confirms the potential of magnetic immobilization for industrial-scale bioethanol production.

5. Conclusions

Fe_3O_4 magnetic nanoparticles were successfully synthesized by co-precipitation, subsequently coated with SiO_2 and functionalized with amine groups, enabling the immobilization of *S. cerevisiae*. Characterization confirmed the formation and functionalization of the material, evidenced by the positive zeta potential and characteristic spectral bands of Fe_3O_4, SiO_2, and $–NH_2$ groups. Orange bagasse proved to be a promising biomass for obtaining fermentable sugars, achieving conversions of up to 90% in 48 h under conditions of pH 4.5 and 30 °C. The application of magnetic nanoparticles as a support allowed the reuse of the yeast for up to six fermentation cycles, with consistent performance, especially at 72 h. Although the ethanol yield with immobilized yeast was lower than that obtained with free yeast, it is important to highlight that studies exploring the use of functionalized magnetic nanoparticles as a support for cell immobilization in fermentation processes are still scarce. In this context, this approach represents an innovative strategy with high technological potential, offering advantages such as easy recovery and reuse of the biocatalyst. Thus, the main objective of this study was to demonstrate the viability of using this technology, which was successfully achieved, evidenced by the ability of the MNP@yeast system to perform fermentation and produce ethanol. The results indicate that this technology constitutes a promising alternative, which can be further explored and optimized, especially through adjustments in operating conditions, such as pH and temperature, aiming to maximize process yield.

Supplementary Materials: The following supporting information can be downloaded at the website of this paper posted on Preprints.org.

Author Contributions: Neidelênio Baltazar Soares: investigation, writing—original draft & editing. Symone Costa de Castro: investigation and analysis. João Guilherme M. Pontes: writing, investigation, and analysis. Ljubica Tasic: science advisor, writing, and review.

Funding: This work was supported by the Coordination for the Improvement of Higher Education Personnel (CAPES) for financial support and the granting of scholarships during the master's degree (Process no. 88882.329146/2010-01—UNICAMP—CHEMISTRY).

Data Availability Statement: The data presented in this study are available on request from the corresponding author.

Acknowledgments: The authors thank the Coordination for the Improvement of Higher Education Personnel (CAPES) for the financial support and granting of scholarships during the master's degree, and the São Paulo Research Foundation (FAPESP) for the funding (Grants #2014/50867-3 and #2022/02992-0) and encouragement of scientific development and infrastructure.

Conflicts of Interest: The authors declare that there is no conflict of interest regarding the publication of this paper.

Abbreviations

The following abbreviations are used in this manuscript:

ADF	Acid detergent fiber
APTES	3-aminopropyltriethoxysilane
CFU	Colony-forming units

 doi:10.20944/preprints202605.1727.v1

FT-IR	Fourier transform infrared spectroscopy
MNPs	Magnetic nanoparticles
NDF	Neutral detergent fiber
OPW	Orange peel waste
TEOS	Tetraethyl orthosilicate
YPD	Yeast Extract-Peptone-Dextrose

References

1. Sales, M.B. Borges, P.T.; Filho, M.N.R.; Silva, L.R.M.; Castro, A.P.; Lopes, A.A.S.; Lima, R.K.C.; Rios, M.A.S.; Santos, J.C.S. Sustainable feedstocks and challenges in biodiesel production: an advanced bibliometric analysis. *Bioengineering* **2022**, *9*(10), 539. DOI: 10.3390/bioengineering9100539.
2. Banco Nacional do Desenvolvimento (BNDES), https://web.bndes.gov.br/bib/jspui/bitstream/1408/2527/1/BS%2025%20Etanol%2C%20Alcoolqu%C3%ADmica%20e%20Biorrefinarias_P.pdf (accessed April 2026).
3. Tiba, S. Revisiting and revising the energy-growth nexus: A non-linear modeling analysis. *Energy* **2019**, *178*, 667. DOI: 10.1016/j.energy.2019.04.116.
4. Opeyemi, B.M. Path to sustainable energy consumption: The possibility of substituting renewable energy for non-renewable energy. *Energy* **2021**, *228*, 120519. DOI: 10.1016/j.energy.2021.120519.
5. Bezerra, M.G. Brandão, M.V.O.R.; Fonseca, E.C.J.; Lima, V.J.A.; Brandão, M.P.; Junior, C.E.A.; Machado, V.; Oliveira, C.S.; Coelho, R.S.; Alves, C.T. Enhancing second-generation ethanol production through acid hydrolysis and *Saccharomyces cerevisiae* fermentation: a sustainable approach using Cassava peel and Manipueira biomass. *Chem. Eng. Trans.* **2024**, *110*, 145. DOI: 10.3303/CET24110025.
6. Li, Y.; Sun, H.; Zhang, Y.; Wang, X.; Gao, M.; Sun, X.; Wang, Q. Research progress for co-production ethanol and biobased products. *Ind. Crop Prod.* **2024**, *212*, 118351. DOI: 10.1016/j.indcrop.2024.118351.
7. Tsukamoto, J.; Durán, N.; Tasic, L. Nanocellulose and bioethanol production from orange waste using isolated microorganisms. *J. Braz. Chem. Soc.* **2013**, *24*(9), 1537-1543. DOI: 10.5935/0103-5053.20130195.
8. Alalwan, H.A.; Alminshid, A.H.; Aljaafari, H.A.S. Promising evolution of biofuel generations. Subject review. *Renew. Energy Focus* **2019**, *28*, 127-139. DOI: 10.1016/j.ref.2018.12.006.
9. Patel, A.; Shah, A.R. Integrated lignocellulosic biorefinery: Gateway for production of second generation ethanol and value added products. *J. Bioresour. Bioprod.* **2021**, *6*, 108-128. DOI: 10.1016/j.jobab.2021.02.001.
10. Jarunglumlert, T.; Prommuak, C. Net energy analysis and techno-economic assessment of co-production of bioethanol and biogas from cellulosic biomass. *Fermentation* **2021**, *7*(4), 229. DOI: 10.3390/fermentation7040229.
11. Chen, J.; Zhang, B.; Luo, L.; Zhang, F.; Yi, Y.; Shan, Y.; Liu, B.; Zhou, Y.; Wang, X.; Lü, X. A review on recycling techniques for bioethanol production from lignocellulosic biomass. *Renew. Sustain. Energy Rev.* **2021**, *149*, 111370. DOI: 10.1016/j.rser.2021.111370.
12. Hawaz, E.; Tafesse, M.; Tesfaye, A.; Kiros, S.; Beyene, D.; Kebede, G.; Boekhout, T.; Groenwald, M.; Theelen, B.; Degefe, A.; et al., Bioethanol production from sugarcane molasses by co-fermentation of *Saccharomyces cerevisiae* isolate TA2 and *Wickerhamomyces anomalus* isolate HCJ2F-19. *Ann. Microbiol.* **2024**, *74*, 13. DOI: 10.1186/s13213-024-01757-8.
13. Baudry, G.; Delrue, F.; Legrand, J.; Pruvost, J.; Vallée, T. The challenge of measuring biofuel sustainability: A stakeholder-driven approach applied to the French case. *Renew. Sustain. Energy Rev.* **2017**, *69*, 933-947. DOI: 10.1016/j.rser.2016.11.022.
14. Joshi, J.; Dhungana, P.; Prajapati, B.; Maharjan, R.; Poudyal, P.; Yadav, M.; Mainali, M.; Yadav, A.P.; Bhattarai, T.; Sreerama, L. Enhancement of ethanol production in electrochemical cell by *Saccharomyces cerevisiae* (CDBT2) and *Wickerhamomyces anomalus* (CDBT7). *Front. Energy Res.* **2019**, *7*, 70. DOI: 10.3389/fenrg.2019.00070.
15. Göktaş, M.; Balki, M.K.; Sayin, C.; Canakci, M. An evaluation of the use of alcohol fuels in SI engines in terms of performance, emission and combustion characteristics: A review. *Fuel* **2021**, *286*(2), 119425. DOI: 10.1016/j.fuel.2020.119425.
16. US-Departament Energy, https://afdc.energy.gov/data/10331 (accessed April 2026).

 doi:10.20944/preprints202605.1727.v1

17. Zhuang, X.; Wang, H.; Jiang, S.; Hu, X.; Su, T.; Zhang, X.; Ma, L. A review on the chemo-catalytic conversion of cellulose to bio-ethanol. *Green Chem. Eng.* **2023**, *5*, 276-289. DOI: 10.1016/j.gce.2023.08.002.
18. Rulli, M.C.; Bellomi, D.; Cazzoli, A.; De Carolis, G.; D'Odorico, P. The water-land-food nexus of first-generation biofuels. *Sci. Rep.* **2016**, *6*, 22521. DOI: 10.1038/srep22521.
19. Santos, N.K.; Pasquini, D.; Baffi, M.A. Factors that influence the enzymatic hydrolysis of agricultural wastes for ethanol production: a review. *J. Eng. Exact Sci.* **2022**, *8*(11), 15137. DOI: 10.18540/jcecvl8iss11pp15137-01e.
20. Sharma, B.; Larroche, C.; Dussap, C.G. Comprehensive assessment of 2G bioethanol production. *Bioresour. Technol.* **2020**, *313*, 123630. DOI: 10.1016/j.biortech.2020.123630.
21. Kordala, N.; Walter, M.; Brzozowski, B.; Lewandowska, M. 2G-biofuel ethanol: an overview of crucial operations, advances and limitations. *Biomass Conv. Bioref.* **2024**, *14*, 2983-3006. DOI: 10.1007/s13399-022-02861-y.
22. Cypriano, D.Z.; Silva, L.L.; Tasic, L. High value-added products from the orange juice industry waste. *Waste Manag.* **2018**, *79*, 71-78. DOI: 10.1016/j.wasman.2018.07.028.
23. Magalhães, A.I.; Carvalho, J.C.; Pereira, G.V.M.; Karp, S.G.; Câmara, M.C.; Medina, J.D.C.; Soccol, C.R. Lignocellulosic biomass from agro-industrial residues in South America: current developments and perspectives. *Biofuels Bioprod. Biorefin.* **2019**, *13*(6), 1505-1519. DOI: 10.1002/bbb.2048.
24. Panwar, N.L.; Kaushik, S.C.; Kothari, S. Role of renewable energy sources in environmental protection: A review. *Renew. Sustain. Energy Rev.* **2011**, *15*(3), 1513-1524. DOI: 10.1016/j.rser.2010.11.037.
25. Zoghlami, A.; Paes, G. Lignocellulosic biomass: Understanding recalcitrance and predicting hydrolysis. *Front. Chem.* **2019**, *7*, 874. DOI: 10.3389/fchem.2019.00874.
26. Mujtaba, M.; Fraceto, L.F.; Fazeli, M.; Mukherjee, S.; Savassa, S.M.; Medeiros, G.A.; Pereira, A.E.S.; Mancini, S.D.; Lipponen, J.; Vilaplana, F. Lignocellulosic biomass from agricultural waste to the circular economy: a review with focus on biofuels, biocomposites and bioplastics. *J. Clean. Prod.* **2023**, *402*, 136815. DOI: 10.1016/j.jclepro.2023.136815.
27. Suri, S.; Singh, A.; Nema, P.K. Current applications of citrus fruit processing waste: A scientific outlook. *Appl. Food Res.* **2022**, *2*(1), 100050. DOI: 10.1016/j.afres.2022.100050.
28. Food and Agriculture Organization of the United Nations, https://www.fao.org/3/cb6492en/cb6492en.pdf (accessed April 2026).
29. Yafetto, L.; Odamtten, G.T.; Wiafe-Kwagyan, M. Valorization of agro-industrial wastes into animal feed through microbial fermentation: A review of the global and Ghanaian case. *Heliyon* **2023**, *9*, e14814. DOI: 10.1016/j.heliyon.2023.e14814.
30. Nieto, G.; Fernández-López, J.; Pérez-Álvarez, J.A.; Peñalver, R.; Ros-Berruezo, G.; Viuda-Martos, M. Valorization of citrus co-products: Recovery of bioactive compounds and application in meat and meat products. *Plants* **2021**, *10*(6), 1069. DOI: 10.3390/plants10061069.
31. Tasic, L.; Tsukamoto, J.; Awan, A.T.; Durán, N. BR Patent, BR1020130325856, 2013, Processo de obtenção de bioetanol, esperidina e nanocelulose a partir do bagaço de laranja, Instituto Nacional da Propriedade Industrial (INPI), 2013.
32. Venkateswarulu, T.C.; Bodaiah, B.; Babu, D.J.; Naraya, A.V.; Evangelin, Y. Bioethanol production by yeast fermentation using pomace waste. *Res. J. Pharm. Technol.* **2015**, *8*(7), 841-844. DOI: 10.5958/0974-360X.2015.00137.7.
33. Musa, U.; Garba, M.U.; Mohammed, I.A.; Munir, S.M.; Abdulhamid, A.F.; Eduk, E.P. Solid state fermentation of orange pomace for bioethanol production. *Cov. J. Eng. Technol.* **2018**, *1*(2), 19-27.
34. Patsalou, M.; Samanides, C.G.; Protopapa, E.; Stavrinou, S.; Vyrides, I.; Koutinas, M. A citrus peel waste biorefinery for ethanol and methane production. *Molecules* **2019**, *24*(13), 2451. DOI: 10.3390/molecules24132451.
35. Lahue, C.; Madden, A.A.; Dunn, R.R.; Smukowski Heil, C. History and domestication of *Saccharomyces cerevisiae* in bread baking. *Front. Genet.* **2020**, *11*, 584718. DOI: 10.3389/fgene.2020.584718.
36. Parapouli, M.; Vasileiadis, A.; Afendra, A.S.; Hatziloukas, E. *Saccharomyces cerevisiae* and its industrial applications. *AIMS Microbiol.* **2020**, *6*(1), 1-31. DOI: 10.3934/microbiol.2020001.

 doi:10.20944/preprints202605.1727.v1

37. Sharma, J.; Kumar, V.; Prasad, R.; Gur, N.A. Engineering of *Saccharomy cerevisiae* as a consolidated bioprocessing host to produce cellulosic ethanol: Recent advancements and current challenges. *Biotechnol. Adv.* **2022**, *56*, 107925. DOI: 10.1016/j.biotechadv.2022.107925.
38. Samantaray, B.; Mohapatra, S.; Mishra, R.R.; Behera, B.C.; Thatoi, H. Bioethanol production from agro-wastes: a comprehensive review with a focus on pretreatment, enzymatic hydrolysis, and fermentation. *Int. J. Green Energy* **2024**, *21*(6), 1398-1424. DOI: 10.1080/15435075.2023.2253871.
39. Tse, T.J.; Wiens, D.J.; Reaney, M.J.T. Production of bioethanol—A review of factors affecting ethanol yield. *Fermentation* **2021**, *7*, 268. DOI: 10.3390/fermentation7040268.
40. Dashko, S.; Zhou, N.; Compagno, C.; Piškur, J. Why, when, and how did yeast evolve alcoholic fermentation? *FEMS Yeast Res.* **2014**, *14*(6), 826-832. DOI: 10.1111/1567-1364.12161.
41. Firoozi, F.R.; Raee, M.J.; Lal, N.; Ebrahiminezhad, A.; Teshnizi, S.H.; Berenjian, A.; Ghasemi, Y. Application of magnetic immobilization for ethanol biosynthesis using *Saccharomyces cerevisiae*. *Sep. Sci. Technol.* **2022**, *57*, 777-787. DOI: 10.1080/01496395.2021.1939376.
42. Mohammadi, Z.B.; Zhang, F.; Kharazmi, M.S.; Jafari, S.M. Nano-biocatalysts for food applications; immobilized enzymes within different nanostructures. *Crit. Rev. Food Sci. Nutr.* **2023**, *63*(32), 11351-11369. DOI: 10.1080/10408398.2022.2092719.
43. Arana-Peña, S.; Carballares, D.; Morellon-Sterlling, R.; Berenguer-Murcia, Á.; Alcántara, A.R.; Rodrigues, R.C.; Fernandez-Lafuente, R. Enzyme co-immobilization: Always the biocatalyst designers' choice…or not? *Biotechnol. Adv.* **2021**, *51*, 107584. DOI: 10.1016/j.biotechadv.2020.107584.
44. Muller, C.; Neves, L.E.; Gomes, L.; Guimarães, M.; Ghesti, G. Processes for alcohol-free beer production: a review. *Food Sci. Tech.* **2020**, *40*(2), 273-281. DOI: 10.1590/fst.32318.
45. Woo, W.X.; Tan, J.W.; Tan, J.P.; Luthfi, A.A.I.; Abdul, P.M.; Manaf, S.F.A.; Yeap, S.K. An insight into enzymatic immobilization techniques on the saccharification of lignocellulosic biomass. *Ind. Eng. Chem. Res.* **2022**, *61*(30), 10603-10615. DOI: 10.1021/acs.iecr.2c01154.
46. A. Ebrahiminezhad, S. M. Taghizadeh, Y. Ghasemi, A. Berenjian, Immobilization of cells by magnetic nanoparticles. In: *Immobilization of Enzymes and Cells*: *Methods and Protocols.* Guisan, J.M.; Bolivar, J.M.; López-Gallego, F.; Rocha-Martín, J.; Eds.; Springer Nature, 2020, pp. 427-435. DOI: 10.1007/978-1-0716-0215-7_29.
47. Dandan, H.; Weiting, Y.; Demeng, Z.; Lili, Z.; Xiudong, L.; Xiaojun, M. Culture of yeast cells immobilized by alginate-chitosan microcapsules in aqueous-organic solvent biphasic system. *J. Oceanol. Limnol.* **2019**, *37*(3), 863-870. DOI: 10.1007/s00343-019-8126-9.
48. Kourkoutas, Y.; Bekatorou, A.; Banat, I.M.; Marchant, R.; Koutinas, A.A. Immobilization technologies and support materials suitable in alcohol beverages production: a review. *Food Microbiol.* **2004**, *21*(4), 377-397. DOI: 10.1016/j.fm.2003.10.005.
49. Mariño, M.A.; Fulaz, S.; Tasic, L. Magnetic nanomaterials as biocatalyst carriers for biomass processing: immobilization strategies, reusability, and applications. *Magnetochemistry* **2021**, *7*(10), 133. DOI: 10.3390/magnetochemistry7100133.
50. Tessarolli, B.O.; Silva, P.V.; Gallardo, E.C.; Magdalena, A.G. Synthesis and characterization of the Fe_3O_4@SiO_2 nanoparticles. *Rev. Materia* **2019**, *24*(4), 1-6. DOI: 10.1590/S1517-707620190004.0831.
51. Mariño, M.A.; Moretti, P.; Tasic, L. Immobilized commercial cellulases onto amino-functionalized magnetic beads for biomass hydrolysis: enhanced stability by non-polar silanization. *Biomass Convers. Biorefin.* **2023**, *13*, 9265-9275. DOI: 10.1007/s13399-021-01798-y.
52. Bouabidi, Z.B.; El-Naas, M.H.; Zhang, Z. Immobilization of microbial cells for the biotreatment of wastewater: A review. *Environ. Chem. Lett.* **2019**, *17*, 241-257. DOI: 10.1007/s10311-018-0795-7.
53. Cheng, G.; Xing, J.; Pi, Z.; Liu, S.; Liu, Z.; Song, F. α-Glucosidase immobilization on functionalized Fe_3O_4 magnetic nanoparticles for screening of enzyme inhibitors. *Chin. Chem. Lett.* **2019**, *30*(3), 656-659. DOI: 10.1016/j.cclet.2018.12.003.
54. Sajjad, A.; Hussain, S.; Jaffari, G.H.; Hanif, S.; Qureshi, M.N.; Zia, M. Fabrication of Hematite (α-Fe_2O_3) nanoparticles under different spectral lights transforms physio chemical, biological, and nanozymatic properties. *Nano Trends* **2023**, *2*, 100010. DOI: 10.1016/j.nwnano.2023.100010.

 doi:10.20944/preprints202605.1727.v1

55. Oberacker, P.; Stepper, P.; Bond, D.M.; Höhn, S.; Focken, J.; Meyer, V.; Schelle, L.; Sugrue, V.J.; Jeunen, G.J.; Moser, T.; et al., Bio-on-magnetic-beads (BOMB): open platform for high-throughput nucleic acid extraction and manipulation. *PLOS Biol.* **2019**, *17*(1), e3000107. DOI: 10.1371/journal.pbio.3000107.
56. National Renewable Energy Laboratory, https://docs.nrel.gov/docs/gen/fy13/42618.pdf (accessed April 2026).
57. Association of Official Analytical Chemists (AOAC), https://www.aoac.org/wp-content/uploads/2019/08/app_f.pdf (accessed April 2026).
58. ANKOM technology Methods, https://www.ankom.com/sites/default/files/document-files/Method_8_Lignin_in_beakers.pdf?srsltid=AfmBOoozfwE-TKa-oeCUiWx8XaA9OyOUF3ykevfpqAnpyvMuWek__g4I (accessed April 2026).
59. Li, W.; Xiao, F.; Bai, X.; Xu, H. Magnetic nanoparticles for food hazard factors sensing: synthesis, modification and application. *Chem. Eng. J.* **2023**, *465*, 142816. DOI: 10.1016/j.cej.2023.142816.
60. Fulaz, S.; Scachetti, C.; Tasic, L. Enzyme-functionalised, core/shell magnetic nanoparticles for selective pH-triggered sucrose capture. *RSC Adv.* **2021**, *11*(8), 4701-4712. DOI: 10.1039/D0RA09259B.
61. da Silva, A.S.; dos Santos, J.H.Z. Stöber method and its nuances over the years. *Adv. Colloid Interface Sci.* **2023**, *314*, 102888. DOI: 10.1016/j.cis.2023.102888.
62. Ding, H.L. Zhang, Y.X.; Wang, S.; Xu, J.M.; Xu, S.C.; Li, G.H. Fe_3O_4@SiO_2 core/shell nanoparticles: The silica coating regulations with a single core for different core sizes and shell thicknesses. *Chem. Mater.* **2012**, *24*(23), 4572-4580. DOI: 10.1021/cm302828d.
63. Vamvakas, S.S.; Kapolos, J. Factors affecting yeast ethanol tolerance and fermentation efficiency. *World J. Microbiol. Biotechnol.* **2020**, *36*(8), 114. DOI: 10.1007/s11274-020-02881-8.
64. Vasconcelos, J.; Lopes, C.; França, F. Continuous ethanol production using yeast immobilized on sugar-cane stalks. *Braz. J. Chem. Eng.* **2004**, *21*(3), 357-365. DOI: 10.1590/S0104-66322004000300002.
65. Lin, Y.; Zhang, W.; Li, C.; Sakakibara, K.; Tanaka, S.; Kong, H. Factors affecting ethanol fermentation using *Saccharomyces cerevisiae* BY4742. *Biomass Bioenergy* **2012**, *47*, 395-401. DOI: 10.1016/j.biombioe.2012.09.019.
66. Queiroz, E.L.; Almeida, T.B.; Silva, A.K.C.; Annunciation, A.S.; Souza, S.M.A.; Martinez, E.A. Optimization of the fermentation process for mead production: a review. *Cuadernos de Educación y Desarrollo* **2024**, *16*(1), 3103-3133. DOI: 10.55905/cuadv16n1-162.